JOURNAL OF CATALYSIS 116, 350–360 (1989)

Geometric Causes of the Methylcyclopentane Ring Opening Selectivity over Pt/NaY Catalysts

GIULIANO MORETTI[1] AND WOLFGANG M. H. SACHTLER[2]

V. N. Ipatieff Laboratory, Center of Catalysis and Surface Science, and Department of Chemistry, Northwestern University, Evanston, Illinois 60208

Received July 6, 1988; revised October 20, 1988

The hydrogenolytic ring opening of methylcyclopentane (MCP) is catalyzed by Pt and other transition metals. The relative rates of cleaving each of the five C–C bonds depend on both chemical and geometric factors. Two preparations of Pt in NaY show different patterns of ring opening products, which are possibly related to the geometry of Pt particles inside the zeolite supercage. If the Pt particles are smaller than the cages, MCP molecules are adsorbed on the Pt particle, but rollover is sterically hindered. In this situation *n*-hexane formation is reduced. If the Pt particle is larger, 3-methylpentane is formed in larger-than-statistical quantities, which may be due to a preferred orientation of the impinging molecule. Ring opening is suppressed by benzene or cyclohexene, i.e., products of the simultaneous ring expansion in catalysts containing an acidic function besides platinum.

INTRODUCTION

In previous research our group has studied the genesis of platinum particles in zeolite NaY, prepared by ion exchange of $Pt(NH_3)_4^{2+}$ ions, followed by temperature-programmed calcination and reduction (*1–6*). It was found that the size and location of reduced platinum particles depend on the calcination and reduction conditions. In these studies, the samples were characterized by several techniques including temperature-programmed reduction (TPR), temperature-programmed desorption (TPD) and extended X-ray absorption fine structure (EXAFS). In conjunction with earlier data obtained by several groups, in particular Gallezot *et al.* (*7–9*), we concluded that four types of reduced Pt particles can be identified in NaY. Of potentially greater importance is that the synthesis steps of such catalysts can be directed toward predominant formation of one of these types of platinum clusters. The objective of "catalyst synthesis by design" appears to be reasonable for these systems. Under conditions where high-activation-energy processes such as zeolite lattice collapse or Ostwald ripening can be disregarded, the major types of Pt clusters and the mechanism of their formation can be described in the following simplified manner:

Pt clusters located inside supercages and of dimensions smaller than these cages. These clusters are obtained by using a calcination program which first strips the Pt^{2+} ions of their NH_3 ligands, but retains the bare Pt^{2+} ions inside the supercages. Upon reduction, small primary Pt clusters are formed which migrate through the wide apertures and coalesce with each other, until the resulting Pt particles are larger than the cage windows and are trapped in their cages, without filling them completely (*2–6*).

Large Pt crystals on the external surface of the zeolite. These are formed by first calcining the sample under severe condi-

[1] On leave from Centro di Studio del CNR SACSO, Chemistry Department, University La Sapienza, Rome, Italy.

[2] To whom correspondence should be addressed.

0021-9517/89 $3.00

tions, driving the Pt^{2+} ions quantitatively into the sodalite cages. Upon subsequent reduction at high temperatures, Pt^0 atoms are formed which leave these cages. They migrate through the channels and, in the absence of appropriate nucleation sites, they form large crystals at the external surface of the zeolite (*3–6*).

Isolated Pt atoms in sodalite cages. If severe calcination is followed by relatively mild reduction, the Pt ions inside sodalite cages are reduced without leaving these cages. These isolated atoms can be reoxidized to Pt^{2+} ions by reacting with protons. This is evidenced by H_2 evolution at high temperature and by a concomitant decrease in the IR intensity of the OH absorption band (*6*).

Pt particles inside the zeolite, but of dimensions larger than the supercage. A calcination program can be defined which strips all Pt^{2+} ions of their NH_3 ligands, but retains part of the bare ions in the supercages, while the rest migrate to sodalite cages. During reduction the Pt^{2+} ions in the supercages are reduced first; they form clusters of type A. By then increasing the reduction temperature further, the Pt^{2+} ions in the sodalite cages become reduced and eventually leave these cages. When these migrating atoms encounter the type A clusters they become trapped. As a result, the type A particles grow further, until they fill their supercage completely or even bulge into neighboring cages (*4–6*). Gallezot *et al.* describe such particles as "grape-shaped." In a previous paper (*10*) we have used this procedure for preparing PtCu particles in NaY; by initially depositing Pt ions in supercages and Cu ions in sodalite cages, we attempted to produce "cherry"-type particles consisting of a Pt core and a Cu mantle.

Isolated Pt atoms in sodalite cages (type B) are catalytically inactive because they are not easily accessible to molecules. In addition, large particles (type C) are of limited interest. The present work, therefore, focuses on the other two types. The following idealized model serves as a working hypothesis for the catalytic action of the two types of catalysts considered:

Type A particles do not fill their supercages. Molecules can enter these cages and become adsorbed. Further reaction is subject to the geometric constraint of the narrow space between particle surface and cage ceiling. Type D particles fill their cages completely; however, in view of the large window sizes, adsorption of molecules is possible only at these windows or on the extensions of the particles into neighboring supercages. As the geometric constraints are different for these two types of particles, a different stereoselectivity might be expected for catalysts predominantly having either A- or D-type Pt clusters.

The present work was undertaken to verify experimentally whether specific differences in stereoselectivity can be identified for Pt/NaY samples with Pt particles predominantly displaying the geometry of either type A or type D. As a catalytic probe we chose the ring opening of methylcyclopentane (MCP). This reaction had been used by Gault (*11*) and other authors, including Chow *et al.* (*12*), Paal (*13*), and Kramer and Zuegg (*14*), to study the effect of metal dispersion and metal/support interaction on the selectivity for the three products: *n*-hexane (*n*-Hex), 2-methylpentane (2-MP), and 3-methylpentane (3-MP). If each of the five C–C bonds in the MCP ring were ruptured with equal probability, the product distribution would be *n*-Hex : 2-MP : 3-MP = 2 : 2 : 1. Deviations from this "statistical distribution" reveal specific effects of the catalyst on the reaction mechanism. For Pt/Al_2O_3 catalysts, Gault *et al.* found that the distribution was nearly statistical for high metal dispersions, but a larger 3-MP/*n*-Hex ratio was observed for samples with low Pt dispersion. Gault *et al.* attribute this to the occurrence of two mechanisms: a "nonselective mechanism," for which the active site might be one Pt atom, and a "selective mechanism" possibly catalyzed by an ensemble of two contig-

uous Pt atoms. Kramer and Zuegg (*14*) found that the product distribution also depends on the nature of the support. They proposed that nonselective mechanism of Gault *et al.* occurs at the phase boundary between Pt particles and support. In this "adlineation" mechanism a reaction is assumed to take place at adjacent metal and support sites located at the phase boundary. The reaction product on this site pair is assumed to be mainly *n*-hexane. Similar results are reported by Anderson *et al.* (*15*) for the Pt/TiO_2 catalyst: an increased selectivity for the formation of *n*-hexane is attributed to a reaction at the metal/titania interface, possibly involving adsorption at a $Pt–Ti^{3+}$ site.

For zeolite-supported Pt, Chow *et al.* (*12*) found that even at a very high Pt dispersion the 3-MP/*n*-Hex ratio was ≈1; i.e., the formation of *n*-Hex was a factor of 2 lower than the statistical value. This was attributed by Jiang *et al.* (*2*) to the geometric constraints of Pt particles which are located in supercages, but do not fill these cages, i.e., type A particles in the above terminology. MCP molecules on such Pt particles are unable to "roll over"; therefore, the C–H bond at the tertiary C atom can dissociate only in 50% of the adsorption events, where this H atom points toward the metal.

Deviations from statistical distribution have usually been observed and discussed for *n*-Hex, i.e., the molecule formed by dissociating the tertiary–secondary C–C bond in the MCP ring. Formation of both 2-MP and 3-MP requires bisecondary C–C bond fission; these products are therefore expected in the statistical ratio 2-MP/3-MP = 2/1. Most published data, in general, roughly confirm this expectation. The 2-MP/3-MP ratio is found nearly 2 for highly dispersed Pt, somewhat larger than 2 for Pt of low dispersion, and between 2 and 3 for Rh/Al_2O_3 and Rh/SiO_2 (*16*). We, therefore, were quite surprised when recent results (*10, 12, 17*) of this laboratory with certain bimetal/zeolite combinations showed 2-MP/3-MP values significantly lower than 2. Table 1 gives an overview of data which were obtained for MCP ring opening with NaY-supported samples tested under identical conditions of temperature and pressure. The results seem to reveal a preference for the formation of 3-MP over and above the statistical value. As these bond fissions involve chemically identical, viz., secondary, carbon atoms, the data suggest that in this case site geometry might affect product distribution. Product selectivity induced by differences in diffusivity can be safely ruled out for these monobranched isomers. The data suggest that the 2-MP/3-MP ratio is 2 for Pt particles of type A, but tends to become smaller than 2 for type D particles which completely fill their supercages. However, as all type D particles in Table 1 consist of two metals, the data are inconclusive because the possibility that the presence of the second metal affects the product distribution cannot be excluded. The present work, therefore, compares the product distributions for type A and type D particles which consist of one metal only, viz., Pt.

TABLE 1

2-MP/3-MP Ratio in MCP Ring Opening over NaY-Supported Mono- and Bimetal Catalysts at Atmospheric Pressure, 250°C, and H_2/MCP = 18

Metal	*r*(particle)/*r*(cage)	2-MP/3-MP	Reference
Pt	<1	2.0–2.2	Chow *et al.* (*12*)
Pt–Cu	>1	1.3–1.5	Moretti and Sachtler (*10*)
Pt–Re	>1	1.4	Nacheff (*17*)

EXPERIMENTAL

Sample Preparation

Two catalysts were prepared: Pt/NaY with Pt loadings of 2.4 and 4.8 wt%. Preparation started with NaY zeolite Linde (LY-Y52) from Union Carbide. The approximate unit cell formula is $Na_{56}(AlO_2)_{56}(SiO_2)_{136}$. The Pt ions were exchanged from an aqueous solution of $Pt(NH_3)_4Cl_2$ (Matheson) containing about 200 ppm of Pt. The exchange was done at 80°C for 12 hr, add-

ing dropwise the necessary amount of solution to the NaY slurry, under vigorous stirring and maintaining a ratio of 1 g of zeolite per 100 ml of solution. The exchanged zeolite was filtered and washed until no Cl^- was detectable.

The catalysts were calcined in O_2 from room temperature to the final temperature, T_C = 300, 360, 450, 550°C, at a heating rate of 0.5°C/min and a flow rate of 1000 ml/min/g of catalyst. They were then kept at T_C for 2 hr in O_2 and 1 hr in Ar or He. The sample color right after calcination is greenish black for the 2.4 wt% catalyst calcined at 300°C and light gray for the others.

The Pt/NaY 4.8 wt% sample was prepared in two steps. After the first ion exchange, the sample was calcined to T_C = 550°C in order to position Pt ions in the sodalite cages. The sample was then cooled and a second ion exchange was performed, followed by a calcination to T_C = 300°C. Quantitative analysis of Pt was done by atomic absorption of the solutions before and after ion exchange. The two samples contained 2.1 and 4.2 Pt atoms per unit cell, respectively.

XRD

X-ray diffraction (XRD) patterns of the samples after the calcination step and after reduction in H_2 were recorded by means of a Rigaku X-ray diffractometer using Cu*K* radiation (Ni filtered). The spectrum of pure NaY, recorded under the same experimental conditions, was used as reference.

XPS

x-Ray photoelectron (XPS) spectra were taken on an ESCALAB spectrometer with Al*K* or Mg*K* radiations working at constant transmission energy (50 eV). The binding energy reference was chosen as the Si(2*p*) line at 102.9 eV (*12*). Samples were prepared by pressing the zeolite in a stainless-steel die. The Pt/NaY samples were studied after calcination and after TPR/TPD experiments. The spectra were accumulated in a multichannel pulse height analyzer and then analyzed using a computer program for smoothing, background subtraction, and curve fitting of the peaks. The samples after TPR/TPD experiments were rereduced for 5 min in H_2 at 500°C in the ESCALAB cell to eliminate the effect of air exposure and then transferred to the analysis chamber in the UHV condition.

TPR/TPD

The apparatus used for the TPR and TPD analysis has been described in a previous paper (*18*). Calcined catalysts were cooled to −80°C in Ar and then changed to 5% H_2 in Ar for TPR at a flow rate of 25 ml/min and a heating rate of 8°C/min up to 530°C. TPD spectra were recorded in flowing Ar after the reduced catalysts had been cooled to room temperature in H_2/Ar. The parameters used are the same as for the TPR experiment.

H_2 Chemisorption

Dispersion measurements by H_2 chemisorption at room temperature were carried out in a vacuum system with a Datametric pressure transducer whose reference side was evacuated at 10^{-5} Torr. The calcined catalysts were reduced in flowing H_2 at the reduction temperature, T_R 300, 450, 500°C, for 2 hr. The samples were then purged in Ar for 15 min at the reduction temperature, cooled to room temperature, and evacuated at 10^{-5} Torr. H_2 was admitted and its pressure increased from 30 to 180 Torr. After determination of the isotherm for total adsorption, the samples were evacuated at room temperature, and a second adsorption isotherm was measured. The difference between the two adsorption measurements, extrapolated to zero pressure, represents the strong H_2 chemisorption. The dispersion is then conventionally defined as the ratio of strongly chemisorbed hydrogen atoms to Pt atoms.

Catalytic Tests

Methylcyclopentane conversion was car-

ried out in a continuous-flow microreactor at atmospheric pressure as described previously (*12*). After reduction in H_2 at T_R 300, 450, 500°C, the catalysts were cooled in H_2 to the reaction temperature. Cooling the sample in He to the reaction temperature does not affect the activity or the selectivity. The conditions were 250°C, flow rate 50 ml/min, H_2/MCP ratio about 18.

With Pt/NaY containing 2.4 wt% Pt, calcined and reduced at 300°C, MCP conversion was also studied in the presence of cyclohexene (cHe) and cyclohexane (cHa). The composition of the gas phase (in Torr) was H_2 : MCP : cHe = 725 : 27 : 8 and H_2 : MCP : cHa = 728 : 20 : 12, respectively.

All the reaction mixtures were generated by bubbling H_2 through a saturator kept at 0°C in an ice bath. MCP is from Baker (Baker Analytical Reagent), cyclohexene from Aldrich (Gold label), and cyclohexane from Mallinckrodt (Analytical Reagent). The reagents were further treated with 5A molecular sieve to remove traces of water.

The amount of zeolite used in every experiment was about 0.1 g. Total conversion was kept below 20%. Reaction products were analyzed with an on-line HP 5794A gas chromatograph equipped with a 50-m crosslinked methyl silicone fused silica capillary column and a flame ionization detector.

RESULTS AND DISCUSSION

X-Ray Diffraction

XRD patterns of the samples were recorded after calcination at T_C 300, 360, 450, 550°C, and after reduction in H_2 for 2 hr at T_R 300, 450, 500°C.

The spectra for the samples after calcination were identical to the spectra of NaY. For the reduced samples with 2.4 wt% Pt, the Pt(111) reflection was detected only for the sample for which T_C = 550°C and T_R = 500°C. These results are in agreement with previous results obtained in our lab with Pt/NaY samples containing about six Pt atoms per unit cell (*3, 5, 6*).

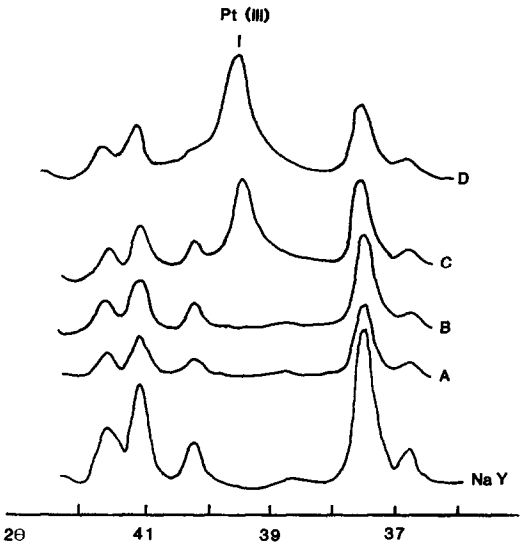

FIG. 1. XRD patterns of NaY and Pt/NaY 2.4 wt% (A–C) and 4.8 wt% (D) after H_2 reduction for 2 h. Sample pretreatments: (A) T_C = 300°C, T_R = 450°C; (B) T_C = 450°C, T_R = 500°C; (C) T_C = 550°C, T_R = 500°C; (D) T_C = 300°C, T_R = 300°C.

The sample containing 4.8 wt% shows the Pt(111) reflection after calcination at 300°C and reduction in H_2 at 300°C. In Fig. 1 are shown the XRD spectra of a selected series of samples after calcination and reduction at different temperatures.

For the two samples for which the Pt(111) reflection is detectable, the average Pt particle size obtained by the Scherrer formula is 200 Å. However, it should be noted that the dispersions (D = H/Pt) are very different (see below): for the 2.4 wt% sample, D = 0.20; for the 4.8 wt% catalyst D = 0.60. This result strongly suggests that in the case of Pt/NaY 4.8% wt%, small platinum particles are entrapped in the supercages while large particles are supported on the external surface of the zeolite matrix.

Considering the detection limit of the technique, all other samples contain Pt metal particles less than 40 Å in size.

XPS Analysis

After calcination in O_2 at 300°C the 2.4 wt% Pt sample presents a Pt($4f_{7/2}$) peak at

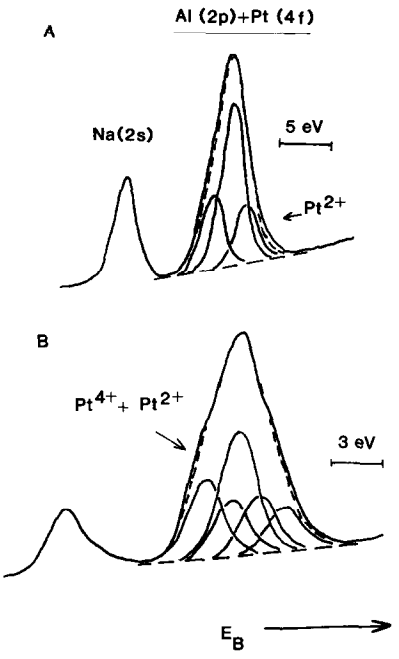

FIG. 2. Curve fitting of Al(2*p*) and Pt(4*f*) peaks for Pt/NaY 2.4 wt% (A) and 4.8 wt% (B) samples after calcination at 300°C. The Pt(4*f*) peak is a doublet ($4f_{7/2}$ and $4f_{5/2}$) due to spin-orbit splitting.

the binding energy E_B = 73.2 eV indicating the presence of Pt^{2+} (*19*). For the sample with 4.8 wt% Pt two peaks are present, one at 73.2 eV and the other at 74.8 eV, indicating that in this case both Pt^{2+} and Pt^{4+} are present. The fraction of Pt^{4+} calculated from the area of the peaks is about 40%. In Fig. 2 are shown the XPS spectra of the calcined samples. The parameters used for the curve fitting were the same for both spectra. The presence of Pt^{4+} has also been confirmed by TPR (see below).

After reduction in H_2 at 300°C, Pt^0 is formed as shown by the Pt($4f_{7/2}$) peak at E_B = 71.7 eV in both samples, irrespective of the metal dispersion. This is in agreement with the results reported by Védrine *et al.* (*19*).

From the intensity ratios and the cross sections reported by Schofield (*20*) atomic ratios Pt/Si, Na/Si, and Al/Si can be calculated. For the calcined samples they are equal within 15% to the values of the chemical analysis. The results are reported in Table 2.

TPR and TPD Spectra

Pt/NaY 2.4 wt%. The TPR and the TPD spectra for this sample after calcination are shown in Fig. 3. The results are in agreement with previous studies performed in this lab on more concentrated samples containing 4.8 to 9.4 Pt atoms per unit cell (*3–6*).

The temperature required to completely reduce all Pt ions increases with calcination temperature (T_C). For all samples the area under the curve indicates that each Pt ion requires two hydrogen atoms to be reduced, which implies that all Pt ions in this sample remain in the divalent state as in the original complex. This is also confirmed by our XPS results.

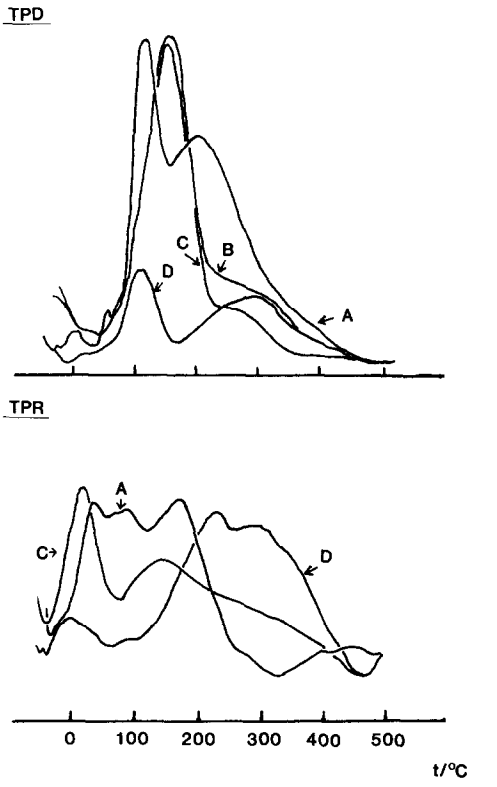

FIG. 3. TPR and TPD spectra for Pt/NaY 2.4 wt% samples after calcination in O_2. T_C = (A) 300°C, (B) 360°C, (C) 450°C, (D) 550°C.

TABLE 2

Atomic Ratios Determined by XPS for Pt/NaY Samples after Calcination at 300°C

Sample	Na/Si	Al/Si	Pt/Si
Pt 2.4 wt%	0.36	0.35	0.018
Theoretical	0.38	0.41	0.015
Pt 4.8 wt%	0.29	0.35	0.034
Theoretical	0.35	0.41	0.030

As was found previously (*3–6*) and summarized in the Introduction to the present paper, calcination at 300°C leaves all Pt ions in the supercages, but at higher calcination temperature they start migrating into the sodalite cages. At T_C = 550°C this migration is complete; therefore a higher temperature is required for their reduction. The low-temperature peaks (from 0 to 200°C) in Fig. 3 thus correspond to reduction of Pt ions in supercages, and the high-temperature peaks to reduction of Pt ions in sodalite cages (*6*). Metal dispersions derived from the integrated TPD spectra are listed in Table 3. As expected, the highest dispersion of 1.0 is observed for the preparation geared toward type A particles, i.e., T_C = T_R = 300°C. Based on previous results (*6*), we assume that the Pt particles in these samples are located inside supercages and that they are larger than the cage window (7.5 Å), but smaller than the cage diameter (13 Å).

After calcination at moderately high temperatures (360–450°C) Pt ions are known to be distributed over supercages and sodalite cages. The ions in the supercages are reduced first, forming small metal particles, which then act as nucleation sites where Pt atoms coming out of the sodalite cages are trapped (*3–6*). This preparation should thus lead to type D Pt particles. Indeed, the measured dispersion near 70% corresponds to an average size of 20–30 Å, in agreement with this model.

A very low dispersion of 25% is observed for those preparations (T_C = 550°C, T_R = 500°C) for which previous data predict that type B particles are formed at the external surface. Accordingly, a strong Pt(111) reflection peak is detected by XRD.

Pt/NaY 4.8 wt%. The TPR and TPD results for this sample are reported in Fig. 4. A new TPR peak is present at about 530°C. H_2 consumption shows that about 40% of the platinum was oxidized to Pt^{4+}. This is in agreement with the XPS data, and it reflects the effect of the unusual preparation method, as no Pt^{4+} was detected for the other samples. The peak positions have been discussed in (*4–6*). We suggest that reduction of Pt^{4+} to Pt^0 in sodalite cages occurs in two steps. Previous EXAFS results of Pt/NaY samples with high metal loading indicated that after calcination at high temperature, two platinum ions are present in the same sodalite cage (*6*). We assume that in this peculiar preparation procedure Pt^{2+} ions were oxidized to Pt^{4+} during the second calcination following the second ion exchange.

When the TPR is stopped at 530°C the TPD spectra of these samples show a peak

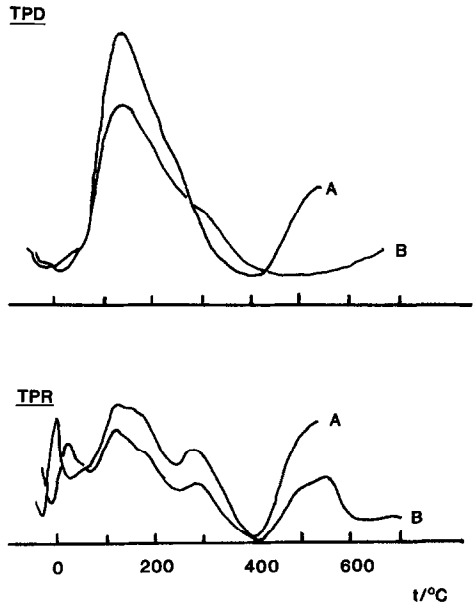

FIG. 4. TPR and TPD spectra for the Pt/NaY 4.8 wt% sample after calcination in O_2 at 300°C. (A) TPR terminated at 530°C; (B) TPR terminated at 700°C.

TABLE 3

Platinum Dispersion D (= H/Pt) of Pt/NaY 2.4 wt% Sample Calcined and Reduced under Different Experimental Conditions[a]

T_C (°C)	T_R (°C)	D = H/Pt
300	300	1.0
300	450	0.79
300	500	—
360	500	0.69
450	500	0.64
550	500	0.2

[a] T_C = calcination temperature. T_R = reduction temperature.

at high temperature. Previously it has been shown (*6*) by FTIR that this release of H_2 is due to oxidation of Pt atoms in the sodalite cages by hydroxyl groups, i.e., the protons that had been formed when Pt^{2+} was reduced with H_2. This reversal of the original reduction reaction is, therefore, not a true desorption of adsorbed hydrogen; consequently, this peak has to be disregarded in determining the metal dispersion. A similar reoxidation of metal atoms in sodalite cages or hexagonal prisms was also found with Ni/NaY (*21*) and with Cu/NaY (*10*). If temperature-programmed reduction is continued up to 700°C, the platinum atoms leave the sodalite cages and, consequently, the TPD peak characteristic of reoxidation of metal atoms in small cages is absent.

The dispersion of the 4.8 wt% Pt/NaY sample after reduction at 300°C is $D = 0.60$. This value is obtained by integrating the TPD spectrum, disregarding the high-temperature peak. As mentioned above, comparison of this dispersion with the particle size value calculated from the XRD linewidth indicates a bimodal distribution of Pt particle sizes.

H_2 Chemisorption

H_2 chemisorption data for the catalyst Pt/NaY 2.4 wt% which had been calcined and reduced under different experimental conditions are reported in Table 3. The measured H/Pt values, conventionally termed "Pt dispersion" are used to calculate the turnover frequency (TOF) of MCP conversion. As outlined above, Pt dispersion decreases with increasing *calcination* temperature. For a given T_C of 300°C the data in Table 3 indicate that Pt dispersion decreases with increasing *reduction* temperature.

MCP Conversion

TOFs for the 2.4 wt% Pt catalysts, calculated from the total conversion after 5 min on stream, are reported in Fig. 5 as a function of Pt dispersion. TOF decreases by a factor of about 2 when the dispersion decreases from 0.80 to 0.20. TOFs obtained for the catalysts with high metal dispersion agree with previous results obtained in this lab on Pt/NaY and Pt/SiO_2 (*12*). A similar trend of TOF with metal dispersion (or particle size) has been reported for Pt on amorphous supports (*14, 15*).

The selectivity ratios 2-MP/3-MP and 3-MP/*n*-Hex are plotted in Fig. 6 against Pt dispersion. For the sample with low metal dispersion, i.e., prevailing type B particles, the 3-MP/*n*-Hex ratio is in agreement with the results reported by Gault (*11*) for Pt/

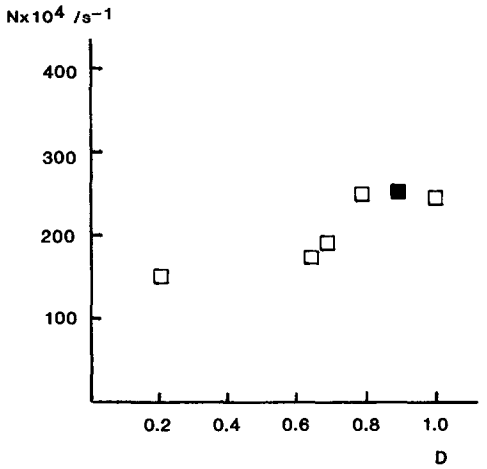

FIG. 5. Turnover frequencies for MCP conversion on Pt/NaY 2.4 wt% catalysts at 1 atm, H_2/MCP = 18, and 250°C as a function of Pt dispersion D. Data after 5 min on stream. Solid point from Chow *et al.* (*12*).

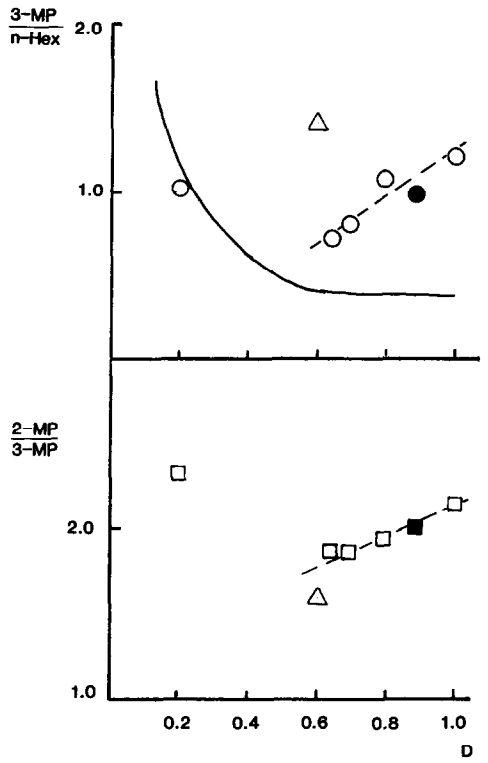

FIG. 6. 2-MP/3-MP and 3-MP/*n*-Hex molar ratios as a function of Pt dispersion D on Pt/NaY 2.4 wt% catalysts. Gault's results for 3-MP/*n*-Hex versus D are represented by the solid line. The solid points represent data by Chow *et al.* (*12*). Δ = 4.8 wt% Pt sample, prepared by second ion exchange after calcination.

Al_2O_3; also, the 2-MP/3-MP ratio of this sample is in the range covered by literature data for Pt on amorphous supports. This agrees with our expectation: large type B particles at the external surface do not reflect the geometry of zeolite cages. For Pt/Al_2O_3 catalysts with high dispersion, Gault found a statistical product distribution for the ring opening products. The present results reported in Fig. 6 for Pt/NaY show a different pattern, and the following observations can be made:

1. The 3-MP/*n*-Hex ratio at high dispersion (D = 1) exceeds the statistical value by a factor of about 2, in agreement with previous results by Chow *et al.* (*12*). With decreasing Pt dispersion 3-MP/*n*-Hex decreases toward the statistical value.

2. The 2-MP/3-MP ratio of about 2.2 is close to the statistical value for high Pt dispersion and in agreement with earlier experimental results (*12*); the ratio decreases with decreasing metal dispersion to a value of 1.8. This deviation from the statistical value is significant; the experimental error for the selectivity ratios is estimated to be less than 3%.

For the 4.8 wt% Pt/NaY sample a bimodal distribution of the metal particle size is indicated by the TPD and XRD results. The high 3-MP/*n*-Hex ratio observed for this sample might be rationalized by assuming that the large particles supported on the external surface of the zeolite matrix play a major role in the MCP ring opening. In the terminology of Luck *et al.* (*22*) this ratio corresponds to a relative contribution of the selective mechanism of about 64%.

As pointed out in the Introduction, interest in this research is primarily focused on the 2-MP/3-MP ratio. The 2-MP/3-MP ratio of 1.8, which we observe for samples with low Pt dispersion, is not only significantly lower than the statistical value, but deviates even more from the experimental data for Pt/Al_2O_3 with low dispersion, for which Gault (*11*) reports values higher than 2. As it is reasonable to assume that Pt particles on the external surface of the zeolite will display the same behavior as Pt/SiO_2, it follows that the metal particles entrapped *in* the zeolite produce much more 3-MP than Pt particles of the same size supported on alumina or silica. It is remarkable that the value for our 4.8 wt% Pt catalyst is even lower, viz., 1.6; this sample was specially prepared with the goal of maximizing the content of type D particles which fill their supercages completely or even bulge into adjacent cages. It appears safe to conclude that such particles are characterized by a 2-MP/3-MP ratio significantly lower than the statistical value. Note that the observed value is still an upper limit for the value characteristic of type D; any type B particles present in the same sample produce a 2-MP/3-MP ratio greater than 2; the charac-

teristic number for type D particles is, therefore, 1.6 or lower.

Since chemical interaction between the reduced metal and the zeolite is known to be weak, a rationalization of the observed selectivity ratios in terms of the geometry of the metal particles inside the zeolite channel system appears justified along the lines outlined in the Introduction.

The lower-than-statistical ratio of *n*-Hex formation on Pt/NaY with high metal dispersion was previously ascribed to the geometric constraints for MCP adsorbed on a Pt particle that incompletely fills the supercage (*2*). As discussed there, only in 50% of the approaches of an MCP molecule will the hydrogen atom at the tertiary carbon be pointing toward the metal surface, so that the Pt–C (tertiary) bond can be formed which is required for ring opening to produce *n*-Hex. In the other 50%, rollover is necessary for *n*-Hex formation to occur. This rollover is impossible in the narrow slit between Pt particle and cage ceiling. A consequence of this simple model is that the deviation from statistics should disappear when the metal particles become larger and fill the cage completely or bulge into adjacent cages. No geometric constraints will then impede rollover of molecules adsorbed at the exposed part of the metal particle. This is just what is observed for decreasing dispersion of Pt particles entrapped in the zeolite, as shown in Fig. 6.

As mentioned in the Introduction, the 2-MP/3-MP ratio is even more relevant for the microgeometry of the catalyst system, because only secondary C atoms are involved. This ratio is less than 2 when the metal particles completely fill the cage in which they are located. This result can also be rationalized in geometric terms. The MCP molecule has a length/width ratio of about 1.7. Before it reaches a metal particle it has to diffuse through the narrow pore system of the zeolite and will probably be oriented with its long axis parallel to the pore axes. If the molecule enters a cage partially filled with a type A particle, adsorption may be followed by α, β stepping over, and memory of the original orientation will be lost. However, the impact of an oriented molecule on the Pt atoms exposed at the cage window of a type D particle might lead to a less flexible adsorption complex retaining the Pt–C bonds formed first. Ring opening can then occur only when the impinging molecule is oriented toward the metal with its flat bottom end. The preferred product thus becomes 3-MP. The present observation that the 2-MP/3-MP ratio decreases with decreasing dispersion is in agreement with this model. Further support is provided by the very low 2-MP/3-MP ratio found with the preparation geared toward maximizing type D particles. It should be mentioned that orientation of hydrocarbon molecules in zeolites has also been proposed by Tauster and Steger (*23*) as a potential cause of stereospecificity in a reaction catalyzed by metal particles in the zeolite.

MCP ring opening is strongly suppressed in the presence of cyclohexene or cyclohexane in the gas feed. The MCP conversion after 5 min on stream decreases from about 16% with pure MCP, to about 1% with both mixtures. Cyclohexane and cyclohexene are rapidly dehydrogenated to benzene; in both cases the benzene/cyclohexane ratio is about 0.07, i.e., near equilibrium under our experimental conditions.

Previously it had been found (*12*) that introduction of an acidic function into Pt/NaY not only opens an additional reaction channel for converting MCP to C_6 ring products but also deactivates the catalyst for MCP ring opening at 250°C. This observation is explained by the present result: the C_6 ring products contain benzene in a concentration given by equilibrium with cyclohexane and H_2, and this benzene blocks the Pt sites suppressing the adsorption of MCP at 250°C virtually completely.

CONCLUSIONS

Several conclusions emerged from this study.

The microgeometry of the metal/zeolite

system can explain the observed selectivity ratios for MCP conversion over Pt/NaY without invoking any particular interaction between the metal particles and the support. Only the metal function is responsible for the ring opening activity.

For metal particles smaller than the diameter of the supercages, the 3-MP/*n*-Hex ratio is two times the statistical value, presumably because of the rollover limitation.

Whereas for Pt supported on alumina, silica, magnesia, or titania, literature consistently reports that MCP ring opening yields hexane isomers with a 2-MP/3-MP ratio exceeding the statistical value of 2, Pt/NaY appears to be unique, as a 2-MP/3-MP ratio significantly lower than 2 is found for the first time. This result is tentatively ascribed to a higher-than-statistical formation of 3-MP due to the orientation of MCP molecules impinging on Pt particles which fill their supercage completely or even bulge through the window into the next cage.

Ring expansion over Pt/HY leads to benzene and cyclohexene which block Pt sites for ring opening of MCP at 250°C.

ACKNOWLEDGMENTS

G.M. acknowledges receipt of financial support from the NATO–CNR Advanced Fellowships Program. The authors thank M. S. Tzou for useful discussions.

REFERENCES

1. Park, S. H., Tzou, M. S., and Sachtler, W. M. H., *Appl. Catal.* **24,** 85 (1986).
2. Jiang, H. J., Tzou, M. S., and Sachtler, W. M. H., *Appl. Catal.* **39,** 255 (1988).
3. Tzou, M. S., Jiang, H. J., and Sachtler, W. M. H., *React. Kinet. Catal. Lett.* **35,** 207 (1987).
4. Tzou, M. S., and Sachtler, W. M. H., *in* "*Catalysis* 1987, Proceedings, 10th North American Meeting of Catalysis Society, San Diego, CA, May 17–22, 1987" (J. W. Ward, Ed.), Studies in Surface Science and Catalysis, Vol. 38, p. 233. Elsevier, Amsterdam.
5. Tzou, M. S., Jiang, H. J., and Sachtler, W. M. H., *Solid State Ionics* **26,** 71 (1988).
6. Tzou, M. S., Teo, B. K., and Sachtler, W. M. H., *J. Catal.* **113,** 220 (1988).
7. Gallezot, P., Alarcon-Diaz, A., Dalmon, J.-A., Renouprez, A. J., and Imelik, B., *J. Catal.* **39,** 334 (1975). See also Gallezot, P., *Catal. Rev.* **20,** 121 (1979) and references therein.
8. Gallezot, P., *in* "Metal Clusters" (M. Moskovits, Ed.), p. 219. Wiley, New York, 1986.
9. Gallezot, P., and Bergeret, G., *in* "Catalyst Deactivation" (E. E. Peterson and A. T. Bell, Eds.), p. 263. Dekker, New York, 1987.
10. Moretti, G., and Sachtler, W. M. H., *J. Catal.* **115,** 205 (1989).
11. Gault, F. G., *Adv. Catal.* **30,** 7 (1981) and previous papers by Gault's group quoted therein.
12. Chow, M., Park, S. H., and Sachtler, W. M. H., *Appl. Catal.* **19,** 349 (1985).
13. See Paal, Z., *Catal. Today* **2,** 595 (1988).
14. Kramer, R., and Zuegg, H., *J. Catal.* **80,** 446 (1983); *J. Catal.* **85,** 330 (1984); *in* "Proceedings, 8th International Congress on Catalysis, Berlin, 1984," Vol. 5, p. 275, 1984.
15. Anderson, J. B. F., Burch, R., and Cairns, J. A., *J. Catal.* **107,** 351 (1987).
16. Del Angel, G., Coq, B., Dutartre, R., and Figueras, F., *J. Catal.* **87,** 27 (1984).
17. Nacheff, M., Ph.D. thesis, Northwestern University, 1988.
18. Tzou, M. S., Jiang, H. J., and Sachtler, W. M. H., *Appl. Catal.* **20,** 231 (1986).
19. Védrine, J. C., Dufaux, M., Naccache, C., and Imelik, B., *J. Chem. Soc. Faraday Trans. 1* **74,** 440 (1978).
20. Scofield, J. H., *J. Electron Spectrosc. Relat. Phenom.* **8,** 129 (1976).
21. Jiang, H. J., Tzou, M. S., and Sachtler, W. M. H., *Catal. Lett.* **1,** 99 (1988).
22. Luck, F., Schmitt, J. L., and Maire, G., *React. Kinet. Catal. Lett.* **21,** 219 (1982).
23. Tauster, S. J., and Steger, J. J., *Materials Res. Soc. Symp. Proc.* **111,** 419 (1988).